Chalcogenide Letters Vol. 18, No. 8, August 2021, p. 473 - 479

Excellent flexible Tin Oxide-metal sulfide nanocomposites grown by spin coating chemical route

R. Sharma, V. Kumar, Y. C. Goswami*
School of Sciences, ITM University, Gwalior (M.P.) INDIA-474001

Tin oxide /Metal sulfide nanocomposites were synthesized using two step solution route. In the first step SnO_2 gel were obtained followed by the next step of addition of precursor of cadmium and sulfide salts. Films were grown on cellulose flexible substrate using spin coating method. All the samples were analyzed using structural, morphological and optical characterizations. In X ray diffractograms, tetragonal rutile structure is observed with shift in peak towards lower angle due to tensile strain. SEM micrographs show that the ring like structure converted into flake like structures. AFM micrographs also confirm the ring like or porous film converted into flake. Photoluminescence spectra exhibits the intensity of SnO_2-CdS decreases as compared to SnO_2. Optical transmittance confirms the formation of nanocomposite due to additional band was observed in nanocomposites.

(Received June 9, 2021; Accepted August 20, 2021)

Keywords: Green synthesis, Cadmium Sulfide, Semiconductor, Nanocomposites, XRD

1. Introduction

Tin chloride is a technologically important n- type wide band gap (3.63 eV) semiconducting material [1]. Unique electrical and optical properties [1,2] of SnO_2 in nanostructures form make them promising material for gas sensing, solar cells, transparent electrodes and photo catalysts [3-6] applications. However, the applications of SnO_2 are severely imitated by less stable and short lifetime excitons. The stability can be improved by controlling the surface activity and by increasing lifetime of exciton. As a solution the formation of nanocomposites [7] can be used. Chalcogenide materials CdS has an excellent light collecting ability in the visible region to release the electron [8]. SnO_2–CdS nanocomposites, appear to be one of the most promising material to overcome these limitations. SnO_2-CdS nanocomposites is a type-II heterostructure in which electron transfer from higher conduction band of CdS to low conduction band of SnO_2 and hole reside in the valance band of CdS because the conduction band of SnO_2 is less negative (0.0 V vs NHE) than CdS (-0.8 V vs NHE) [9] results in effective charge separations [10]. SnO_2-CdS nanocomposites results in significant change in structural, optical and surface morphology of SnO_2.Several papers have been reported on SnO_2-CdS heterostructures synthesized using various methods such as hydrothermal, screen printing, colloidal approach, sonochemical approach, chemical vapor deposition and ultrasonic method [11-15] etc. However among various methods sol-gel is favorable, friendly and attractive due to simplicity, low cost and less hazardous (low temperature processing). Moreover, the morphology and properties of SnO_2 – CdS nanocomposites can be controlled by various growth conditions such as temperature, spin rate concentrations and pH of the solution. Apart from this in the modern era of electronics flexibility of device is also an important concern. In the recent past, most of the research was carried out on the rigid substrates like glass, therefore have limited use [16,17]. Recently some papers have been reported on synthesis of tin chloride on various flexible substrate like cellulose acetate, poly (ethylene terephthalate), ITO-PET, PES [18-21]. Out of which Cellulose acetate flexible substrate gained much attraction due to its unique properties including high transparency, good stability, low cost and easily available [22-24]. To the best of our knowledge no work is reported on spin coating of SnO_2-CdS nanocomposites on cellulose acetate flexible substrates. In this paper, we have reported spin coating of SnO_2-CdS nanocomposites on cellulose acetate flexible substrate and their morphological, structural and optical characterizations.

* Corresponding author: ranjanagoswami4@gmail.com

https://doi.org/10.15251/CL.2021.188.473

2. Experimental procedure

Tin chloride dehydrate, ethanol, thiourea and Cadmium chloride of AR grade obtained from the Fisher chemicals were used as starting materials. All the samples were used without further purification. The whole process is divided into three steps: Synthesis of SnO_2 gel, synthesis of SnO_2-CdS nanocomposites and spin coating of SnO_2-CdS nanocomposites on cellulose acetate substrates.

2.1. Synthesis of SnO_2 gel

In the first step, 0.1M of tin chloride was dissolved in 30ml of ethanol and stirred ultrasonically (40 KHz, 1000W) for 1hr at 70^0C. 2ml of HCl was added to prevent from hydrolysis. A transparent sol was obtained which was kept for aging for about 12 hrs finally converted into gel.

2.2. Synthesis of SnO_2-CdS nanocomposites in the solution

In the second step, 0.03M of Cadmium chloride, 0.03M of thiourea and 10ml ethylene glycol mixed together using ultrasonically for 1hr and then slowly added in SnO_2 gel. After 3hrs, light yellow transparent sol was obtained which converted into gel after about 36 hrs aging. The gel was used for spin coating of the thin films on cellulosed acetate flexible substrates.

2.3. Spin coating on cellulose acetate substrates

Spin coater model number APEX-NXG was used for deposition of films. Cellulose acetate sheet supplied by Grafix plastics were used as the flexible substrates. Before deposition the substrates were thoroughly cleaned by water and then acetone. The substrates in the typical size of 1cmx1cm were placed on substrate holder of Spin coater. The composite in the form of gel was transferred to the substrate using micro syringe. The spin rate was initially was kept at 2000 rpm for first 10 seconds and then increases to 6000 for another 30 seconds. The whole process was repeated about 30 times to get required thickness. The samples obtained were annealed at 100^0C for 2hrs.

2.4. Characterization

The samples were analyzed by various techniques for structural, morphological, optical studies using X-ray diffractograms (XRD), Scanning electron microscopy (SEM), Atomic force Microscopy(AFM), photoluminescence (PL) and UV-VIS spectra respectively. X ray diffractograms were recorded using X-Pert Pro, PAN analytical X-ray diffractometer in the 2θ ranging from 20^0 to 70^0 with Cu Kα radiation(λ=1.5406). Å), SEM micrographs were obtained by SX100 (Cameca), AFM micrographs were recorded using digital Instrumentation-Inc, USA contact mode, Optical spectra were obtained using Perkin Elmer λ-25 spectrophotometer ranging from 200nm-900nm and Fluorescence spectra were recorded using Perkin Elmer LS-55 Spectro fluorometer ranging from 200 nm-900 nm.

3. Results and discussion

3.1. Structural Analysis

X-ray diffractograms of bare SnO_2 and SnO_2-CdS nanocomposites on a cellulose flexible substrate are shown in figure 1 (a) and (b). Very Broad peaks observed indicate very small structures. All the peaks in Fig 1 (a) are observed at 26.5^0, 34.6^0, 38^0 and 52^0identified for SnO_2 and indexed as (110), (101), (200) and (211) respectively. These peaks match with the data of tetragonal rutile crystalline structure (JCPDS 41-1445). X ray diffractogram for SnO_2-CdS nanocomposite is shown in Fig 1(b). No peaks of CdS are observed indicates amorphous nature of CdS in the composite. The dominant peak in the curve (110) of sample (b) shifts towards lower

angle due to tensile strain. Similar result reported [25]. At the same time all other peaks are absent indicates a kind of orientation took place in the SnO_2 structure.

The crystallite size is measured using Debye – Scherrer formula [26] for these samples.

$$D = \frac{K\lambda}{\beta cos\theta}$$

where β is the full width at half maxima (FWHM), D is the average crystallite size, λ is the wavelength used in X-ray, $\boldsymbol{\theta}$ is the diffraction angle and K is the shape factor and its value close to unity.

Sample (a) of pure SnO_2 is recorded as 3.98 nm. When CdS compound deposited on SnO_2, the crystallite size of SnO_2-CdS nanocomposites increases upto 8 nm. The strain was calculated by drawing Williamson's Hall plot (W-H Plot) shown in Fig 2. [27] using the equation

$$\beta \cos\theta = \frac{0.9\lambda}{D} + \eta \mathrm{Sin}\theta$$

where β is the full width at half maxima, λ is the wavelength of X-ray used and η is the latticestrain. The strain for SnO_2 and SnO_2-CdS nanocomposites found to be 0.213 and 0.028. The –ve slope shows the tensile strain occurred by the particles and increases in the composite due to inclusion of CdS in pure SnO_2.

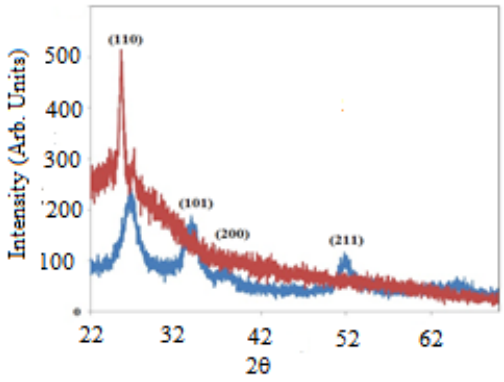

Fig. 1. X-Ray diffraction spectra of (a) pure SnO_2 and (b) SnO_2-CdS nanocomposites

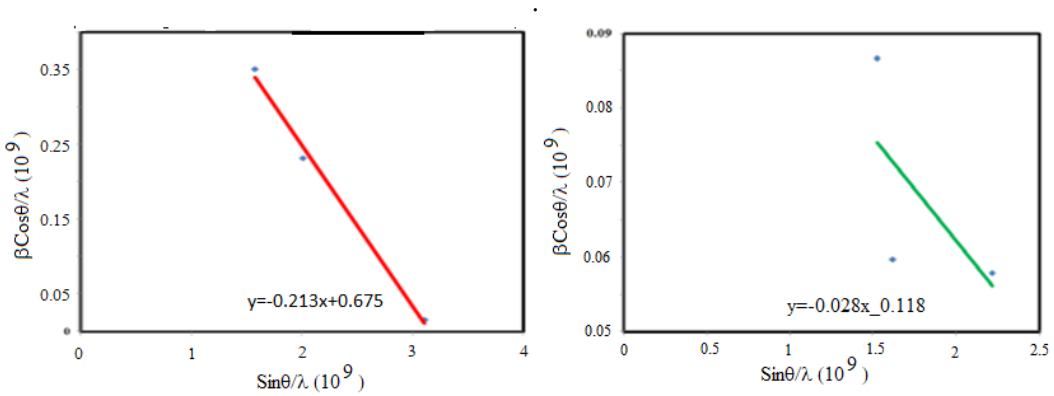

Fig. 2. Williamson's Hall plot (W-H plot) of sample (a) pure SnO_2 and (b) of SnO_2-CdS nanocomposites.

SEM micrographs of bare SnO_2 and SnO_2-CdS nanocomposites are shown in figure 3. Pure SnO_2 of sample (a) show a porous or ring-like structure. The length of pores is about 70nm-80nm. With the deposition of CdS on SnO_2, the rings are converted into flake-like structures. This might be due to inclusion of CdS in the pores network, this also supported by XRD results.

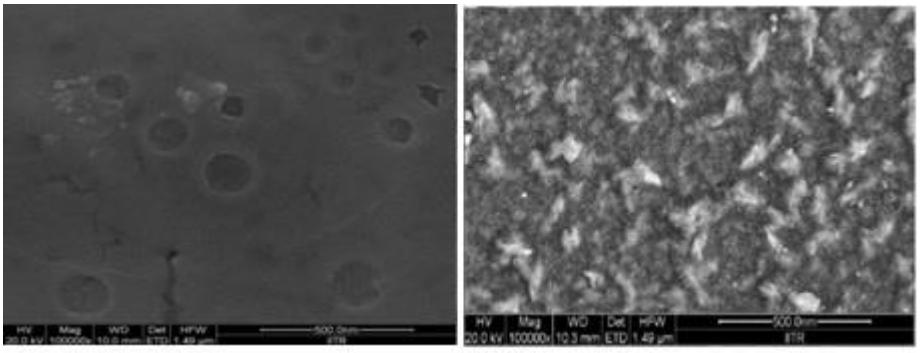

Fig. 3. SEM micrographs of spin coated bare tin oxide and Tin oxide Metal Sulfide nanocomposites.

AFM results matches with theSEM results as shown in figure 4. In figure 4, pure SnO_2 shows porous structure. The depth of porous was estimated as 34nm and height of the selected area was estimated as 15nm. The difference in size estimated by SEM and AFM might be due to different resolution of these techniques. Deposition of CdS, ring structure converted into flake like structure was observed in Fig4(b). The depth was estimated as 8.5nm and height as 3nm in sample 4(b). The roughness of SnO_2-CdS nanocomposites (2.743 nm) decreasing as compared with pure SnO_2makes these structures suitable for various sensing applications [28-29]. The calculated crystallite size, strain and roughness of the SnO_2 and SnO_2-CdS heterostructures are shown in table 1.

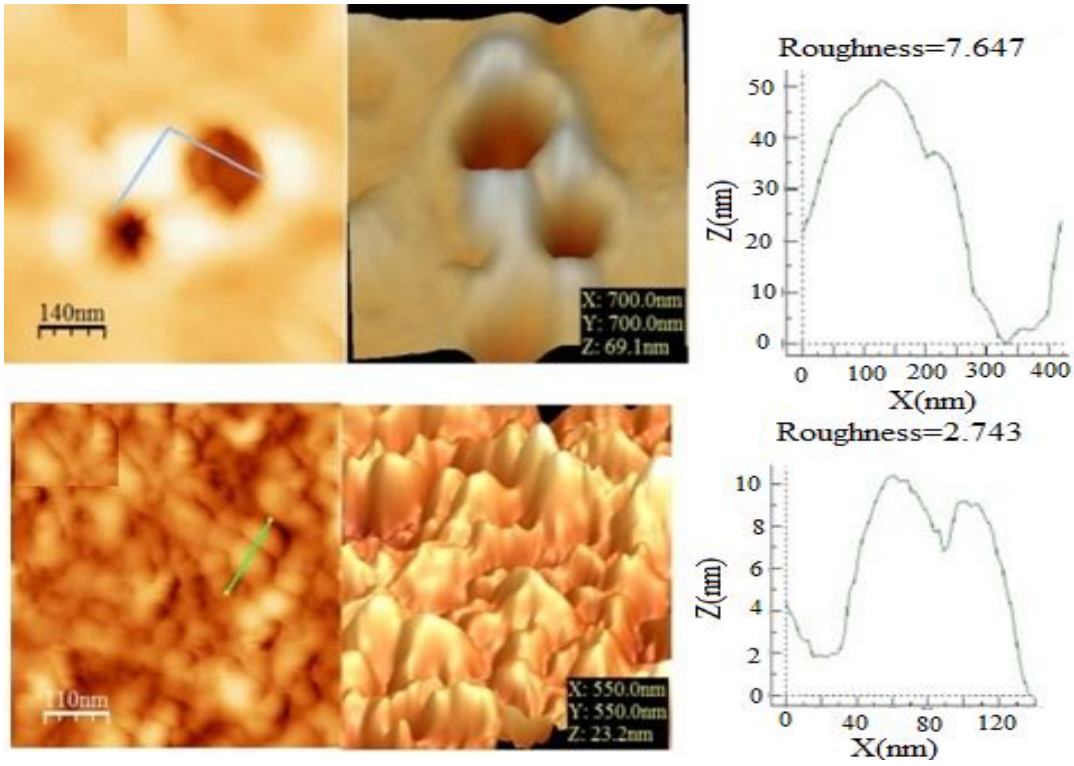

Fig. 4. AFM micrographs of spin coated (a) bare tin oxide and (b) Tin oxide Metal Sulfide nanocomposites.

Table 1. The crystallite size, strain and roughness of the SnO_2 and SnO_2-CdS heterostructures are calculated and shown in table.

S.No.	Sample	Crystallite size (nm)	strain	Roughness (nm)
1	**SnO_2**	3.98	0.213	7.647
2	**SnO_2-CdS**	8	0.028	2.743

Photoluminescence studies were carried out for SnO_2 and SnO_2-CdS nanocomposites shown in figure 5**.**

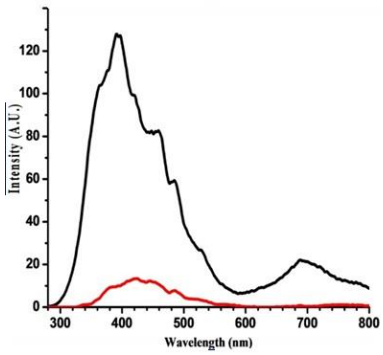

Fig. 5. Photoluminescence spectra of spin coated (a) bare tin oxide Shown in black (b) Tin oxide Metal Sulfide nanocomposites (Shown in red).

Sample (a) of pureSnO_2 shows a strong emission peak at 400 nm. Another peak at 700 nm is also observed due to defect related oxygen vacancies. On deposition of CdS particles on SnO_2,the intensity of peaks in the sample (b) decreases as that of pure SnO_2 and weak emission is observed at 430 nm in sample (b). This observed due to effective charge separation. Peak shift

towards higher wavelength is justified for nanocomposite as the size of the particle increases. The intensity of Tin oxide Metal Sulphide nanocomposites decreases as compared to SnO2 however at higher wavelength the intensity increase might be due to involvement of deeper states.

Optical transmittance spectra of spin coated bare Tin oxide and Tin oxide Metal Sulfide nanocomposites were carried out for SnO_2 and SnO_2-CdS nanocomposites shown in figure 6. Decrease in overall intensity is observed, with observation of two edges corresponds to tin oxide and CdS absorption edges. Peak shifts towards higher wavelength is justified for nanocomposite as the size of the particle increases. This confirms the formation of nanocomposites. Good transmission in visible region suitable for optoelectronic devices.

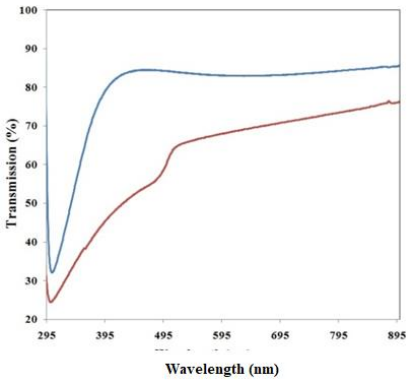

Fig. 6. Optical transmittance spectra of spin coated bare (a) Tin oxide (blue) and (b) Tin oxide Metal Sulfide nanocomposites (red).

4. Conclusions

In this paper, we have first time reported SnO_2-CdS nanocomposites synthesized on a cellulose acetate flexible substrate using spin coating. Shift in X-ray diffraction confirms the formation of nanocomposites due to tensile strain. Scanning electron micrographs show conversion of ring structure into flake-like structures useful for flexible sensing devices. The roughness of SnO_2-CdS nanocomposites decreases as compared with pure SnO_2. Photoluminescence shows a blue shift in nanocomposites and intensity decreases as compared with pure SnO_2. Optical transmittance shows an additional band at 500 nm confirms the formation of nanocomposites. These types of nanocomposites useful for flexible optoelectronic devices.

Acknowledgements

Authors are thankful to MPCST and AICTE for providing the funding. We are also thankful to IUAC, Indore for the facilities of XRD & AFM facilities and IIT Roorki for SEM facility.

References

[1] S. M. Rozati, E. Shadmani, Digest Journal of Nanomaterials and Biostructures 6(2), 365(2011).
[2] A. N. Banerjee, S. Kundoo, P. Saha, K. K. Chattopadhyay, Journal of Sol-Gel Science and Technology 28, 105 (2003).
[3] N. G. Deshpande, Y. G. Gudage, R. Sharma, J. C. Vyas, J. B. Kim, Y. P. Lee, Sensors and Actuators B 138, 76 (2009).
[4] J. Zhu, Z. Lu, S. T. Aruna, D. Aurbach, A. Gedanken, Chemistry of Materials 12(9), 2557 (2000).
[5] S. Ferrere, A. Zaban, B. A. Gregg, J. Phys. Chem. B 101, 4490 (1997).
[6] Y. S. He, J. C. Campbell, R. C. Murphy, M. F. Arendt, J. S. Swinnea, J. Mater. Res. 8, 93.

[7] R. Mohapatra, J. B. Kaundal and Y C Goswami, Chalcogenide letters, 18(5), 255, (2021).
[8] N. Jiang, Z. Xiu, Z.Xie, H. Li, G. Zhao, W. Wang , Y. Wu, X.Hao, New J. Chem. 38, 4312 (2014).
[9] A. Kar, S. Kundu, A. Patra, J. Phys. Chem. C 115, 118 (2011).
[10] H. Sun, S. Z. Kang, J. Mu, Journal of Dispersion Science and Technology 30(3), 384 (2009).
[11] A. Kar, S. Kundu, A. Patra, RSC Adv. 2, 10222 (2012).
[12] X. Meng, F. Wu, J. Li, J. Phys. Chem. C 115, 7225 (2011).
[13] A. Phuruangrat, B. Kuntalue, T. Thongtm, S. Thonetem, Chalcogenide Letters 16(4), 149 (2019).
[14] C. Nasr, P. V. Kamat, S. Hotchandani, J. Electroanal. Chem. 420, 201 (1997).
[15] Vijay Kumar, P.Rajaram, Y. C. Goswami, Advances in Optical Science and Engineering Springer Proceedings in Physics 166, 557 (2015).
[16] P. Rajaram, Y. C. Goswami, S. Rajagopalan, V. K. Gupta, Mater Lett. 54, 158 (2003).
[17] D. Calestani, L. Lazzarini, G. Salviati, M. Zha,Cryst Res Technol. 40, 937 (2005).
[18] Y. C. Goswami, V. Kumar, P. Rajaram, Materials Letters 128, 425 (2014).
[19] G. Gustafsson, Y. Cao, G. M. Treacy, F. Klavetter, N. Colaneri, A. J. Heeger, Nature 357, 477 (1992).
[20] S. Ameen, M. S. Akhtar, H. K. Seo, H. S. Shin, Chemical Engineering Journal 281, 599(2015).
[21] S. Zhan, D. Li, S. Liang, X. Chen, X. Li., Sensors 13, 4378 (2013).
[22] R Bisauriya, D Verma, YC Goswami, Journal of Materials Science: Materials in Electronics 29 (3), 1868 (2017).
[23] Kumar, LP Purohit, YC Goswami, Physica E: Low-dimensional Systems and Nanostructures 83, 333 (2016).
[24] R Sharma, R Singh, YC Goswami, V Kumar, D Kumar, Journal of the Australian Ceramic Society, 1-7
[25] K. Wang, J. J. Chem., W. L. Zhou, Y. Zhang, Y. F. Yan, J. Pern, A. Mascarenhas, Adv. Mater. 20(17), 3248 (2008).
[26] B. D. Cullity, S. R. Stock, Elements of X-Ray Diffraction, 3rd Ed., Prentice-Hall Inc. Canada 167(2001)
[27] C. Suryanarayana, M. G. Norton, X-ray diffraction: a practical approach. Plenum Press, New York, (1998).
[28] Z. G. Li and B. Zeng Chalcogenide Letters Vol. 18, No. 1, 39 – 46 (2021).
[29] N Kumar, LP Purohit, YC Goswami, Chalcogenide Lett 12 (6), 333 (2015).